J Mater Sci: Mater Electron **(2026) 37:449**

Enhanced structures and magnetic properties of $Li_{0.43}Zn_{0.28}Ti_{0.14}Fe_{2.15}O_4$ ferrites co-fired with Bi_2O_3–CaO sintering aid at low temperatures for LTCC applications

Xiaoyi Wang[1,2], Ning Ma[1], Ziyan Yang[1], Hui Li[1], Xiujuan Feng[3,*], Gang Zhou[2], Gang Chen[1], and Lei Zhao[1,*]

[1] *School of Information and Control Engineering, China University of Mining and Technology, Xuzhou 221116, Jiangsu, China*
[2] *Ningbo Sunny Infrared Technologies Co., Ltd, Ningbo 315400, Zhejiang, China*
[3] *National Key Laboratory of Deep Coal Safety Mining and Environmental Protection, Anhui University of Science and Technology, Huainan 232001, Anhui, China*

Received: 16 September 2025
Accepted: 30 January 2026
Published online: 27 February 2026

ABSTRACT

The requirements of miniaturizing microwave devices have brought about vigorous developments in low-temperature co-fired ceramics (LTCC) technology, in which circumstance synthesizing ferrimagnetic materials at low sintering temperatures becomes a crucial part. In this study, $Li_{0.43}Zn_{0.28}Ti_{0.14}Fe_{2.15}O_4$ ferrites were prepared via a solid-state reaction method, with Bi_2O_3–CaO mixture serving as sintering aid. Based on various characterization results, it can be concluded that the introduction of Bi_2O_3–CaO as a sintering aid can achieve the fabrication of Li–Zn ferrites with pure spinel phases at low temperatures. Grain growth and densification were promoted with the assistance of sintering aid with an appropriate addition amount (0.5 wt%). Regarding magnetic properties, the value of saturation magnetic induction increased from 141.3 to 236.7 mT, and value of ferromagnetic resonance linewidth decreased from 1448 to 632 Oe. Thus Bi_2O_3–CaO mixture proves to be an effective sintering aid, which might be applied for LTCC applications.

1 Introduction

Ferrite materials are widely utilized for modern microwave devices (such as phase shifter, circulator, isolator, etc.) owing to their unique properties, and increasing attentions have been paid to them in recent decades [1–3]. Generally, ferrite materials could be divided into three categories: spinel, garnet, and hexaferrite depending on their different crystal structures [4, 5]. Regarding spinel ferrites, a space group of *Fd*3*m* is obtained, and the structure can usually be expressed as AB_2O_4, where A sites represent divalent cations with occupying fourfold tetrahedra and B sites represent trivalent cations with occupying sixfold octahedra [6–8].

Address correspondence to E-mail: fengxj.2011@tsinghua.org.cn; leizhao@cumt.edu.cn

https://doi.org/10.1007/s10854-026-16743-w

Kinds of spinel ferrites have been developed including Mn–Zn, NiCuZn, and Li–Zn ferrites, and most of them have industrial applications [9, 10]. Among them, Li–Zn ferrites are considered good substrate materials for phase shifter because of their excellent magnetic properties including high saturation magnetization and high remanence square ratio, low ferromagnetic resonance linewidth, and low cost [11–13].

On the other hand, device miniaturization is the development trend in the world, which can improve the integration degree of microwave system and reduce energy consumption at the same time. To this end, low-temperature co-fired ceramics (LTCC) technology has been proposed and considered as an effective method [14]. With the assistance of LTCC technology, multilayer hybrid integrated circuits can be produced, where passive components (resistors, inductors, and capacitors) and active components are integrated in the same package [15–18]. Obviously, it is beneficial for microwave wireless applications that high integration and high-performance devices can be achieved. It is worth noting that the melting point of silver is only 960 °C, which is much lower than the sintering temperature of spinel ferrite ceramics with traditional fabricating routes. Therefore, it is a key issue to reduce the sintering temperature in order to realize co-firing of spinel ferrites and silver conductors [19–21].

In this background, fabricating Li–Zn ferrites at low sintering temperatures (less than 950 °C) gradually becomes a research hotspot, and much effort has been made [22]. Adding sintering aid is proved to be a valid approach to achieve the synthesis of Li–Zn ferrites at low temperatures, among which glass and oxides with low melting points are most widely used. For example, Wang et al. fabricated B_2O_3–Li_2CO_3–SiO_2–ZnO glass and employed it as sintering aid to synthesis Li–Zn ferrites at 920 °C [23]. In regard of glass sintering aid, its advantage is the much low melting point. However, the glass needs to be fabricated separately with a complicated procedure, specifically, a relatively complex procedure containing high-temperature calcination, quenching, and pulverization steps. Another kind of sintering aid is oxide or mixed oxides; they only need to be added during the second ball milling process, which can significantly reduce synthesis complexity. At the very beginning, only one type of oxide was added and served as the sintering aid, such as Bi_2O_3, which is one of the most widely used oxide sintering aid [24]. For example, Liu et al. used Bi_2O_3 as sintering aid to prepare LiZn ferrites at low temperatures and investigated the influences [25]. The sintering temperature can be remarkably reduced with the introduction of Bi_2O_3, but other magnetic properties of Li–Zn ferrites can hardly be effectively tailored by only adjusting the proportion of Bi_2O_3. To this end, many scholars focus their attentions on mixed oxides, which can reduce the sintering temperature, and meanwhile adjust specific properties to meet the needs of microwave devices [26, 27].

Herein, Bi_2O_3–CaO mixing oxide was employed as the sintering aid to prepare $Li_{0.43}Zn_{0.28}Ti_{0.14}Fe_{2.15}O_4$ ferrite ceramics at low temperatures. In this condition, no complex fabrication procedure was required relative to the glass-based sintering aid, while the introduction of CaO tailored the magnetic properties of products compared to the Bi_2O_3-only sintering aid. For example, Hossein et al. demonstrated that the addition of CaO could increase the saturation magnetization of Mn–Zn ferrites, owing to the substitution of Ca cations at tetrahedral sites [28]. However, little attention has been paid to the influence of CaO on properties of Li–Zn ferrites. Third, this work aims to prepare Li–Zn ferrites with satisfying performances at low sintering temperatures, and it can be deduced that the introduction of Bi_2O_3–CaO mixing oxide might work. So far, the influence of Bi_2O_3–CaO serving as sintering aid on Li–Zn ferrite has not been reported before. In this paper, crystal structure, morphology, and various magnetic properties of $Li_{0.43}Zn_{0.28}Ti_{0.14}Fe_{2.15}O_4$ ferrites with the different amounts of Bi_2O_3–CaO sintering aid were investigated.

2 Experimental

Li–Zn ferrite ceramics with a stoichiometric formulation of $Li_{0.43}Zn_{0.28}Ti_{0.14}Fe_{2.15}O_4$ were prepared via the solid-state reaction method at a low sintering temperature of 900 °C. Specifically, raw materials (Fe_2O_3, ZnO, TiO_2, and Li_2CO_3) with an analytical grade (Guo-Yao Co., Shanghai, China) were weighed according to the stoichiometric value, and total weight of these powders was 50 g. The powders were mixed with distilled water (DI) with a weight ratio of DI: powders = 1.5: 1, and then a planetary mill (Nanjing Machine Factory, Nanjing, China) was employed to make the slurry uniformly mixed, the mixing time lasted for 250 min with a rotating speed of 260 rpm, and the milling media were zirconium oxide balls.

Then, the mixed slurry was dried in an oven at 80 °C for 24 h, followed by crushing and sieving to obtain powders. A pre-sintering procedure was conducted for those powders at 800 °C for 180 min, and the heating rate was 2 °C/min. Next, various amounts of Bi_2O_3–CaO sintering aid (x wt%, $x = 0$, 0.05, 0.1, 0.2, 0.5, 1.0, and 2.0) were mixed with the pre-sintered powders, followed by the ball milling, drying, crushing, and sieving procedures in turn. Finally, those powders were granulated with the help of polyvinyl alcohol (PVA, 10%) and pressed into specific shapes by using a press machine. The prepared samples were sintered at 900 °C in an air atmosphere for 250 min at a heating rate of 2 °C/min, and then the temperature of the muffle furnace was gradually cooled down to 200 °C with a decreasing rate of 2 °C/min and finally naturally cooled to room temperature. It is noted that the muffle furnace was kept at 450 °C for 1 h in the sintering process.

Crystalline structures of the synthesized $Li_{0.43}Zn_{0.28}Ti_{0.14}Fe_{2.15}O_4$ ferrites were characterized by X-ray diffraction (XRD, Bruker D8 Advance, Germany) with Cu Kα radiation source, and the scanning range was $2\theta = 10$–80°. As for morphology of the products, those samples were cut, and the cross-sectional microstructures were studied using a field emission scanning electron microscope (FESEM, Tescan MAIA3, Czech Republic). Densities of the synthesized samples were tested by the classical Archimedes' method. A LakeShore7404 vibrating sample magnetometer (VSM) was used to measure the M–H loops at an externally applied field of − 5000 to 5000 Oe at room temperature. Regarding the measurement of ferromagnetic resonance (FMR) linewidths (ΔH), the prepared Li–Zn products were first crushed and ground to obtain spherical specimens with a diameter of 1 mm, and then those spherical specimens were tested via the perturbation method. Other magnetic properties including saturation magnetic induction (B_s), remanent magnetic induction (B_r), remanence square ratio, and coercivity (H_c) were measured by an Iwatsu BH analyzer (SY8232) with an alternating magnetic field.

3 Results and discussion

Figure 1a shows a typical structure of spinel crystal unit cell; cations located at A sites are surrounded by four oxygen anions (tetrahedra), while cations located at B sites are surrounded by six oxygen anions (octahedra), and they are arranged in a close packed arrangement. In a unit cell, oxygen anions contribute 32 ions to make electrically balance and form a close packed structure. It is acknowledged that spinel ferrites can be divided into 3 types including normal, inverse, and mixed ferrites according to the cations distribution. Moreover, the substitution for ions locating at A or B sites has a significant influence on various properties of spinel ferrites, and many researchers are focusing on this topic. Regarding Li–Zn ferrites, the 8 A sites are usually occupied by Zn^{II}/Fe^{III}, whereas the 16 B sites are filled with Li^{I}/Fe^{III}. As shown in Fig. 1b, the prepared Li–Zn ferrites with different addition amounts of Bi_2O_3–CaO sintering aid all exhibit a pure spinel phase, which could be indexed to the main (220), (311), (400), (422), (511), and (440) planes (JCPDS #37-1471). Besides, intensities of diffraction peaks are increasing with the increase of Bi_2O_3–CaO sintering aid, which could be attributed to the enhancement of crystallinity degree, since the increase of peak height usually indicates an increase in grain size and crystallinity. On the other hand, no diffraction peaks of raw agents including Fe_2O_3, ZnO, TiO_2, and Li_2CO_3 are detected. Taking into account the above results, it can be concluded that the $Li_{0.43}Zn_{0.28}Ti_{0.14}Fe_{2.15}O_4$ ferrites with spinel phases were successfully synthesized at a relatively low temperature. Moreover, no impurity peaks of Bi_2O_3 or CaO are observed from the XRD results, indicating that the introduction of sintering aid brings negligible effects on crystal structure of Li–Zn ferrites. Although all the samples display same spinel phase diffraction peaks, intensities of some diffraction peaks are increasing with the increase amount of Bi_2O_3–CaO sintering aid. Furthermore, Rietveld refinement fitted patterns were investigated and are shown in Fig. 1c. As for the sample sintered with 0.5 wt% Bi_2O_3–CaO sintering aid, the values of R_p, R_{wp}, and χ^2 are 6.99%, 8.40%, and 1.17, respectively, indicating a good fitness. The refinement of XRD results indicate that the calculated diffraction patterns exhibit a high compatibility with experimental data, and the existence of sintering aid has negligible effects on spinel crystalline structure. In a word, Li–Zn ferrites can be well fabricated at low sintering temperatures with the assistance of Bi_2O_3–CaO sintering aid, and the existence of sintering aid has no detrimental influences on spinel phase structures.

As shown in Fig. 2, morphologies of some samples of the prepared $Li_{0.43}Zn_{0.28}Ti_{0.14}Fe_{2.15}O_4$ ferrites are

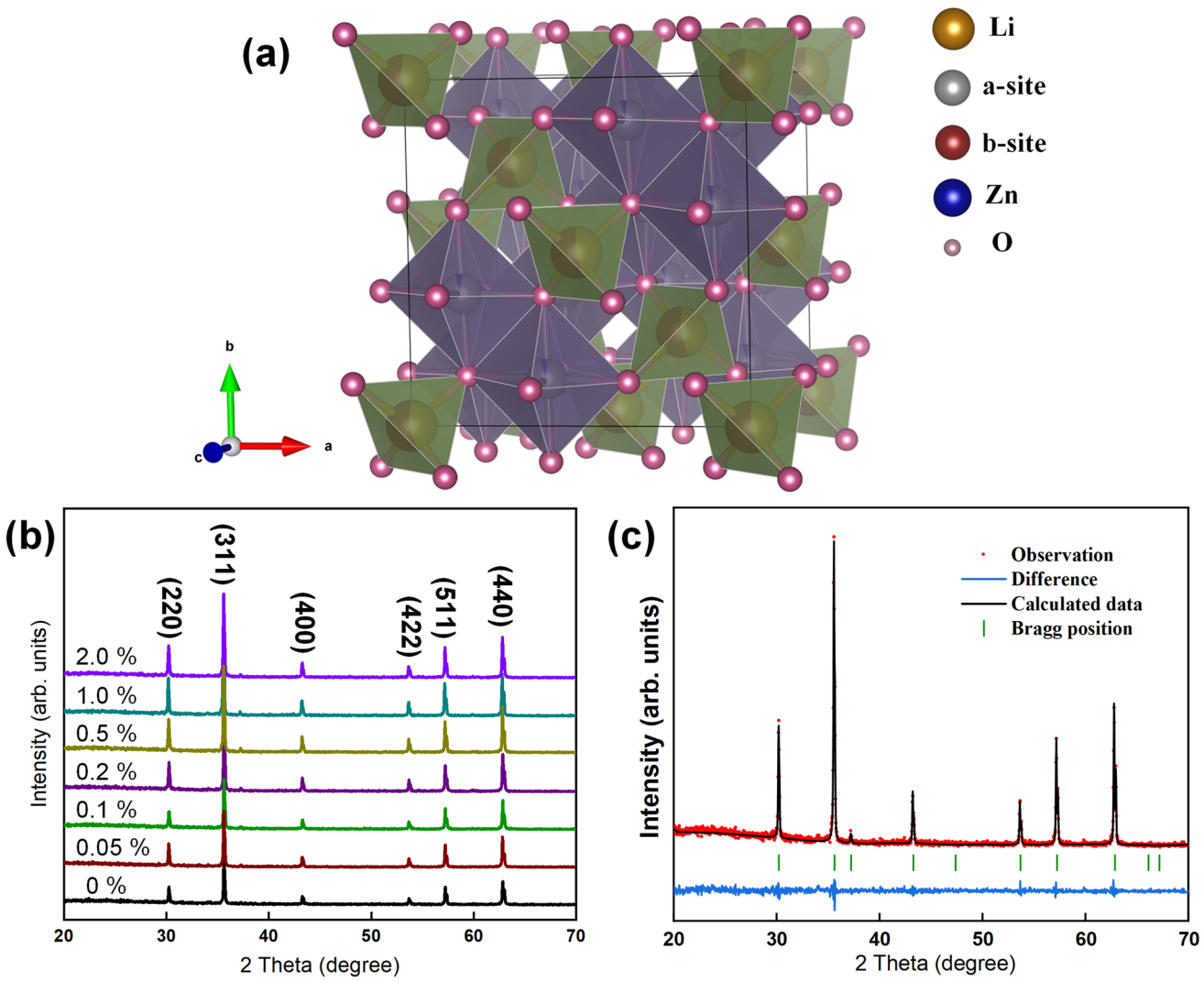

Fig. 1 **a** Schematic illustration of a spinel unit cell. **b** XRD patterns of the prepared Li–Zn ferrites sintered with different amounts of Bi_2O_3-CaO sintering aid. **c** Rietveld refinement results of the sample sintered with 0.5 wt% sintering aid

displayed. Figure 2a, b, c, and d represents the sample sintered with 0 wt%, 0.1 wt%, 0.5 wt%, and 1.0 wt% Bi_2O_3–CaO sintering aid, respectively. In the condition of no sintering aid involved, the grain size is relatively small. The corresponding grain size distribution histograms are shown in Fig. 2 (e), the mean size is only 0.79 μm, and the extremely small grains (0.2–0.4 μm) are very few with only 2% proportion is observed. More than 70% of the grains possess a size range locating at 0.6–1.0 μm, indicating a homogeneous microstructure. Some bigger grains with a size larger than 1.0 μm are less than 10%, which could be attributed to the low sintering temperature, where the growth process is suppressed and the energy of grain movement is insufficient. The above results are not unexpected, which are in consistent with our previous work [29]. Regarding the sample with 0.1% Bi_2O_3–CaO sintering aid introduced, obviously, the densification degree is significantly increased. The average size of the smallest grains is about 1.0 μm (Fig. 2f), and the proportion of grains with an average diameter of around 1.5 μm exceeds 60%. Although the introduction of sintering aid promotes the grain growth, the mean size is still low of 1.45 μm, and no large grains (with a diameter exceeding 2 μm) are detected. It could be explained that the existence of Bi_2O_3 which possesses a low melting point would form liquid phase during the sintering process, and grain growth and migration would be enhanced with the assistance of liquid phase. On the other hand, the addition amount of

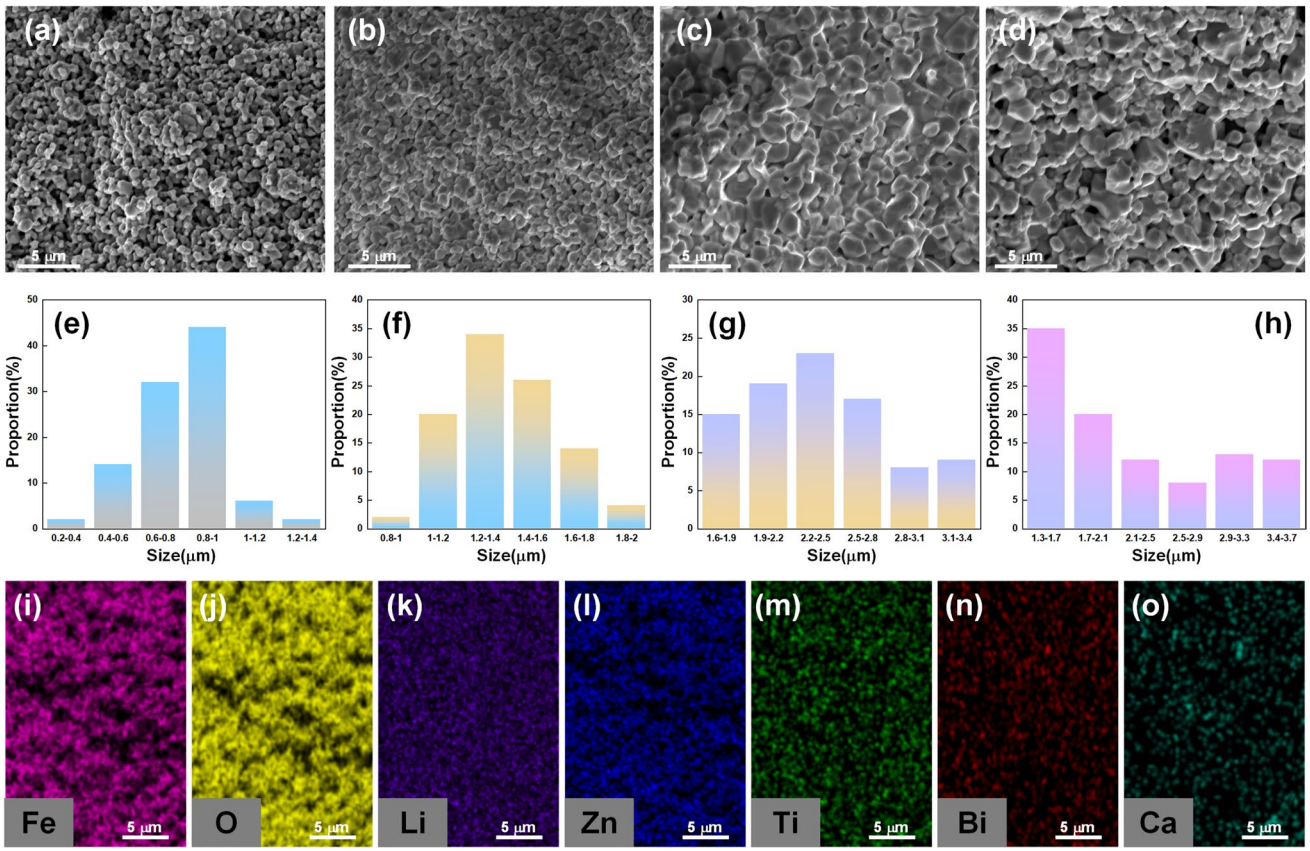

Fig. 2 SEM images and the corresponding size distribution histograms of the samples: **a** and **e** for the 0 wt% sample; **b** and **f** for the 0.1 wt% sample; **c** and **g** for the 0.5 wt% sample; **d** and **h** for the 1.0 wt% sample. **i–o** The mapping results

Bi_2O_3–CaO sintering aid was relatively low, and thus, grain growth was not sufficient. Increasing the amount of sintering aid to 0.5%, mean size of Li–Zn ferrites grains increases to 2.68 μm (Fig. 2g). Under the circumstance, no grains less than 1.5 μm can be observed, more than 80% of the grains possess a diameter larger than 2.0 μm, and some large grains with a diameter of about 3.5 μm emerge. Besides, it can be seen that densification degree is satisfactory, as few pores exist. It is well known that the existence of Bi_2O_3 could facilitate the grain growth because it would become liquid phase during the sintering process owing to its relatively low melting point; however, some abnormally large grains may be formed, and grain conglutination may emerge because of the liquid phase. Herein, CaO was introduced and served as sintering aid to prevent these harmful phenomena owing to its high melting point. During the sintering process, CaO is difficult to be melted into liquid phase, which would inhibit the abnormal growth of grains. Therefore, under the combined effect of Bi_2O_3 and CaO, a better grain growth process was obtained, which would then improve the magnetic properties of Li–Zn ferrites.

Further increasing the amount of sintering aid to 1.0%, uniformity feature is damaged that more small grains are observed and densification degree declines. The grains having a diameter range from 1.3 to 1.7 μm are 35% (Fig. 2h), and grain with an average diameter of around 3.0 μm is 23%, indicating the size distribution is relatively dispersed. The emergence of small grains could be attributed to the excessive amount of Bi_2O_3–CaO sintering aid, in which condition too much liquid phase would deteriorate grain uniformity. EDS mapping is applied along with SEM to analyze the types of elements to provide specimen map, as displayed in Fig. 2i–o, Fe, O, Li, Zn, Ti, Bi, and Ca elements of the prepared Li–Zn ferrites sintered with 0.5 wt% sintering aid are shown, respectively. It can be seen that all the elements of raw materials exist in the final products, and the element distribution is relatively uniform that indicates the well uniformity

of Li–Zn ferrites. In short, Bi_2O_3–CaO sintering aid can promote grain growth and achieve synthesizing Li–Zn ferrites with good microstructures at low sintering temperatures, and the addition amount is a key factor.

Some magnetic properties of the prepared Li–Zn ferrites are displayed in Fig. 3. Figure 3a shows B_s and B_r values of the samples sintered with different contents of Bi_2O_3–CaO sintering aid. Regarding the B_s value, it is significantly increased with the assistance of sintering aid. The B_s value is only 141.3 mT when no sintering aid involved, and then it rapidly increases to 236.7 mT in the condition of 0.2 wt% of Bi_2O_3–CaO added. Further increasing the addition amount to 0.5 wt%, the B_s value can reach up to 279.8 mT, which is nearly twice as much as that of the non-addition sample. It is acknowledged that saturation magnetic induction is remarkably influenced by grains of ferrites, due to the fact that sintering aid would bring about larger grains and higher densification; thus, the B_s values are increased with the increase of addition content. However, B_s value of the sample sintered with 1.0 wt% and 2.0 wt% sintering aid is 264.2 mT and 259.8 mT, respectively. Obviously, B_s values no longer continue to increase but decrease instead. It could be attributed to two factors: first, grain size and densification degree of Li–Zn ferrites decrease when much sintering aid introduced (as can be seen from SEM results); second, both Bi_2O_3 and CaO are non-magnetic materials which will result in a reduction of B_s value. In addition, B_r

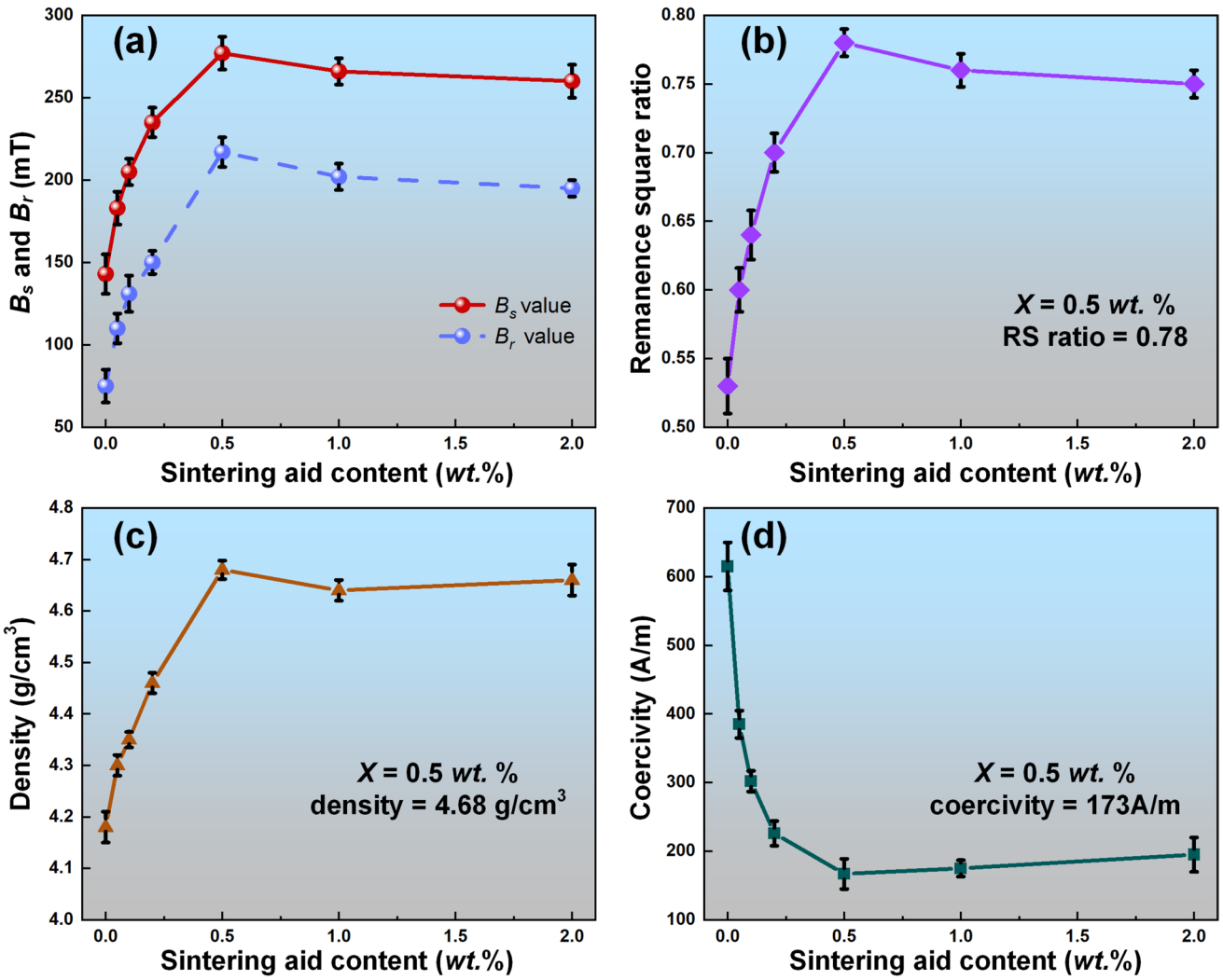

Fig. 3 Values of **a** B_s and B_r, **b** remanence square ratios, **c** densities, and **d** coercivities of the samples sintered with different amounts of Bi_2O_3–CaO sintering aid

values of the samples are displayed via the dotted line. The lowest value is 74.2 mT and it reaches as high as around 218.7 mT in the condition of 0.5 wt% sintering aid involved. Similarly, B_r values also start decreasing when the addition amount exceeding 0.5 wt%, and B_r value of the sample with 2.0 wt% sintering aid is less than 200 mT. Remanence square ratio is an important parameter indicating the degree of rectangularity of hysteresis loop, and large remanence square ratios are desired for magnetic recording materials. Accordingly, remanence square ratios of the samples can be calculated from B_s and B_r results, and they are shown in Fig. 3b. The remanence square ratio is only 0.526 when no sintering aid introduced, and it reaches up to 0.782 when 0.5 wt% sintering aid added. The amplification rate of remanence square ratio is not as large as that of B_s or B_r, because B_s and B_r values are both increasing during this process. Figure 3c shows densities of the samples, since densification degree increases with the increase of sintering aid, density increases from 4.18 g/cm^3 (0 wt%) to 4.68 g/cm^3 (0.5 wt%). Further increasing the addition amount, densities also do not increase, which is in good accordance to microstructure results. Coercivity, also known as magnetic retention force, is the resistance of a magnetic material to changes in magnetization and one of the most important properties of soft magnetic materials, and it represents the ability of magnetic materials to resist demagnetization [30]. Generally, coercivity is influenced by various factors such as grain size, impurities, pores, and defects. Among them, magnitude of coercivity is most strongly affected by the variation of grain size. Therefore, as shown in Fig. 3d, coercivity value dramatically decreases from 617 A/m to 228 A/m when only 0.2 wt% Bi_2O_3–CaO sintering aid added, then it continues decreasing to 173 A/m sintered with 0.5 wt% sintering aid. Since more small grains emerge, coercivity value slightly increases when more than 1.0 wt% sintering aid introduced. Although coercivity value increases in this circumstance, the value of 200 A/m is still much lower than that of the sample without sintering aid. To better compare the effects of different addition amounts on various properties of the Li–Zn ferrites, those results are summarized in Table 1 (Supporting Information). These results verify that grain size is indeed the main influencing factor to coercivity, and on the other hand, we can conclude that the existence of Bi_2O_3–CaO sintering aid can effectively improve magnetic properties of Li–Zn ferrites, and an optimal addition amount is a key.

Room-temperature magnetic hysteresis (M–H) loops of some ferrites samples are displayed in Fig. 4,

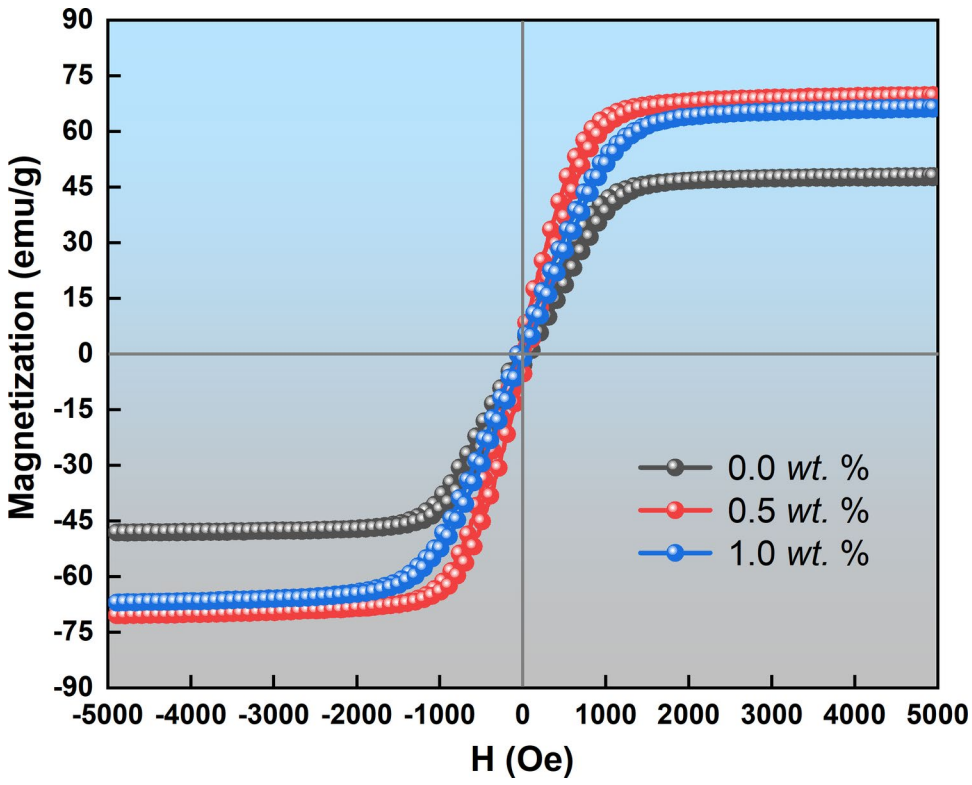

Fig. 4 Hysteresis loops (at room temperature) of the samples co-fired with 0 wt%, 0.5 wt%, and 1.0 wt% Bi_2O_3-CaO sintering aid

and the corresponding magnetization values can be obtained. Clearly, magnetization values of all the samples increase remarkably in the range of 0–1500 Oe, and then they gradually reach a plateau when external magnetic field exceeds 2000 Oe, where the saturation magnetization can be calculated. In the condition of no external magnetic field applied, magnetic domains are oriented in random directions, leading to negligibly small magnetization values. Once external magnetic field introduced, magnetic domains will turn and align parallel to external field, causing obvious increase of magnetization value. Finally, domain walls rotate to the maximum angle they can reach, and thus, magnetization values will not continue increasing, which we call it saturated [31]. The saturation magnetization can be influenced by temperature, stoichiometric formula, and microscopic morphological structure [32]. In this study, Li–Zn ferrites are tested in room temperature; stoichiometric formula is $Li_{0.43}Zn_{0.28}Ti_{0.14}Fe_{2.15}O_4$, and crystal structure has not been destroyed with the addition of Bi_2O_3–CaO sintering aid. Therefore, since microscopic morphological structure will be influenced with different amounts of sintering aid, it is believed to be the most important variable that will affect saturation magnetization. Specifically, saturation magnetization value is only 47.6 emu/g without any sintering aid, and then it can reach up to 69.8 emu/g when 0.5 wt% sintering aid involved. The main reason is that grain growth is promoted and densification degree is enhanced with the assistance of sintering aid, resulting in a higher saturation magnetization value. Nevertheless, saturation magnetization value decreases to 66.4 emu/g in the condition of 1.0 wt% sintering aid added. First, microscopic morphology not only fails to be optimized but deteriorated instead when too much sintering aid introduced. Second, increased proportion of non-magnetic sintering aid will bring about the decline of saturation magnetization.

Ferromagnetic resonance (FMR) is coupling between incident electromagnetic waves and magnetization of the ferrites through which they pass, and FMR linewidths (ΔH) is an important parameter for ferrimagnetic materials. As shown in Fig. 5, FMR spectra of some samples with different amounts of Bi_2O_3–CaO sintering aid are displayed. It can be seen that curves of the samples without (Fig. 5a) or with small addition (0.05 wt%, Fig. 5b) of sintering aids are more gentle than that of the samples sintered with appropriate amount of sintering aids (0.5 wt%, Fig. 5c). The ΔH values of those samples can be calculated; to be specific, a very high value of 1448 Oe is observed for the sample without sintering aid, and then it slightly decreases to 1286 Oe when 0.05 wt% sintering aid involved. In contrast, the ΔH value dramatically decreases to 632 Oe when the sintering aid proportion increases to 0.5 wt%, and it does not continue decreasing (678 Oe) when furthering the sintering aid proportion to 1.0 wt%. Furthermore, the variation of FMR linewidth with Bi_2O_3–CaO sintering aid amount is presented in Fig. S1 (Supporting Information).

Generally speaking, the ΔH value is mainly determined by intrinsic linewidth (ΔH_i), magnetocrystalline-anisotropy induced linewidth (ΔH_k), and porosity-induced linewidth (ΔH_p), and the relationship between them is shown by the formula of $\Delta H = \Delta H_i + \Delta H_k + \Delta H_p$ [33]. It is acknowledged that the value of ΔH_i is much smaller compared with ΔH_k and ΔH_p; for example, Manzoor et al. demonstrated that the ΔH_i value is only about 10 Oe for polycrystalline ferrites, and the corresponding contribution to ΔH value could be ignored [34]. Therefore, it can be concluded that ΔH_k and ΔH_p are the most important parameters that will significantly influence the ΔH value [35, 36]. Based on the SEM and VSM results, the existence of Bi_2O_3–CaO sintering aid could enhance the saturation magnetization and promote the densification degree, which would result in the decrease of ΔH_k and ΔH_p and finally leading to lower ΔH value.

4 Conclusion

In the present work, Li–Zn ferrites were successfully synthesized under low sintering temperatures that are below the melting point of silver, which could be applied for LTCC applications. The introduction of Bi_2O_3–CaO sintering aid played a vital role in the sintering process, in which spinel crystal structures were well maintained. Ferrites grain growth was significantly promoted with the assistance of sintering aid, and average grain size was increased from 0.79 μm (without sintering aid) to 2.78 μm in the condition of 0.5 wt% Bi_2O_3–CaO sintering aid involved. Owing to the large grain size and better densification, some magnetic properties were enhanced. The density

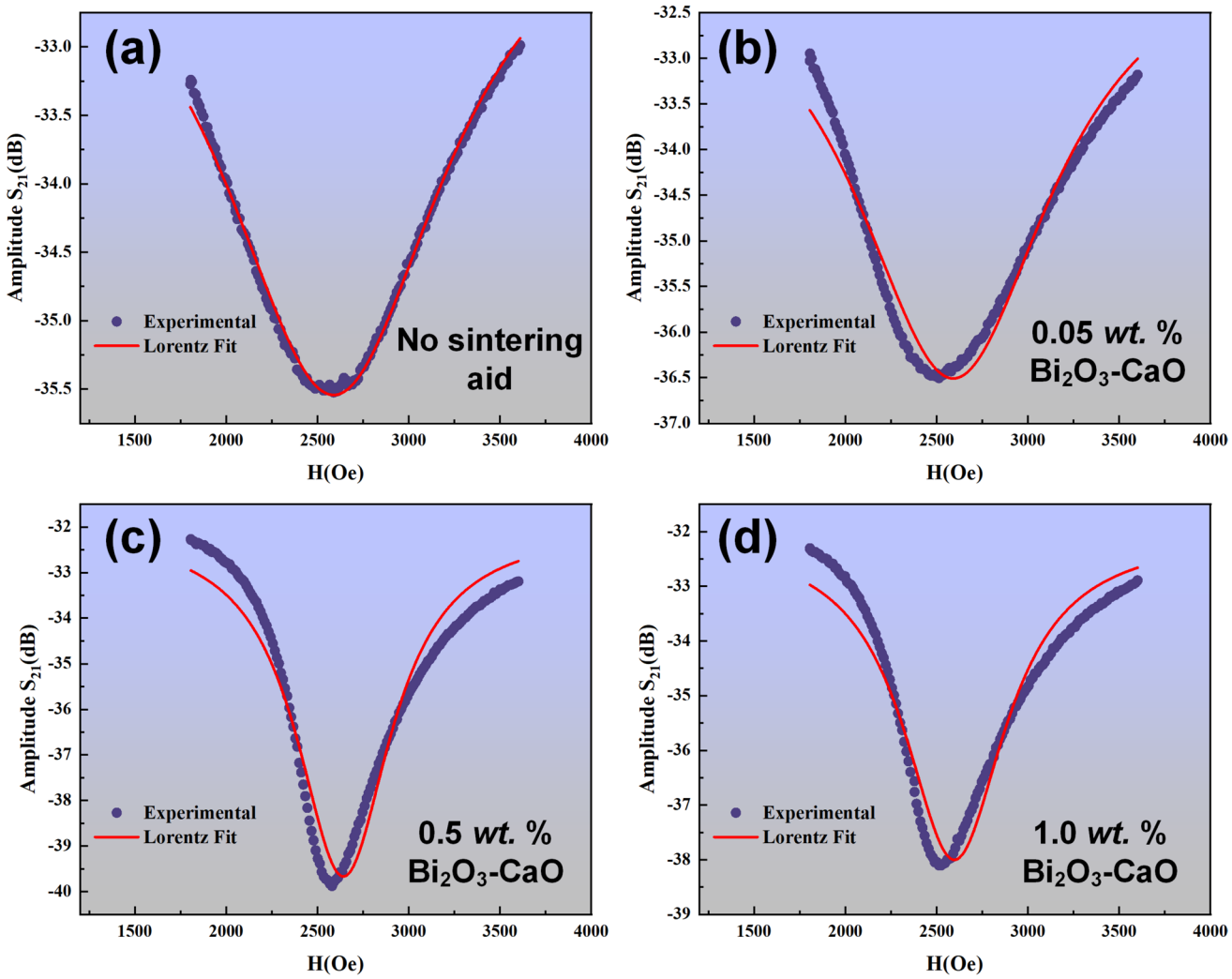

Fig. 5 FMR linewidth of the samples co-fired with **a** 0 wt%, **b** 0.05 wt%, **c** 0.5 wt%, and **d** 1.0 wt% Bi_2O_3–CaO sintering aid

increased from 4.18 g/cm^3 to 4.68 g/cm^3 and B_s value increased from 141.3 mT to 236.7 mT, while ΔH value decreased from 1448 to 632 Oe. In addition, excessive amounts of sintering aid would not continue enhancing the properties of Li–Zn ferrites; in contrast, it might deteriorate some properties. Overall, the existence of Bi_2O_3–CaO sintering aid could achieve the low-temperature fabrication of Li–Zn ferrites and obtain satisfying properties; meanwhile, the synthesis procedure is very convenient. Bi_2O_3–CaO exhibits many advantages compared with that of Bi_2O_3-only or glass-based sintering aids, and it could be a promising candidate for preparing Li–Zn ferrites at low temperatures.

Author contributions

Xiaoyi Wang, Ning Ma, Ziyan Yang and Hui Li wrote the main manuscript text; Xiujuan Feng and Gang Zhou prepared Figs. 1–3; Gang Chen and Lei Zhao prepared Figs. 4–5. All authors reviewed the manuscript.

Funding

This work was supported by the Fundamental Research Funds for the Central Universities (2022QN1051).

Data availability

No datasets were generated or analysed during the current study.

Declarations

Conflict of interest The authors declare no competing interests.

Supplementary Information The online version contains supplementary material available at https://doi.org/10.1007/s10854-026-16743-w.

References

1. V.G. Harris, A. Geiler, Y. Chen, S.D. Yoon, M. Wu, A. Yang, Z. Chen, P. He, P.V. Parimi, X. Zuo, C.E. Patton, M. Abe, O. Acher, C. Vittoria, Recent advances in processing and applications of microwave ferrites. J. Magn. Magn. Mater. **321**, 2035–2047 (2009)
2. R. Valenzuela, Novel applications of ferrites. Phys. Res. Int. **2012**, 591839 (2012)
3. P. Thakur, D. Chahar, S. Taneja, N. Bhalla, A. Thakur, A review on MnZn ferrites: synthesis, characterization and applications. Ceram. Int. **46**, 15740–15763 (2020)
4. V.G. Harris, Modern microwave ferrites. IEEE Trans. Magn. **48**, 1075–1104 (2012)
5. X. Wang, K. Xu, N. Ma, X. Feng, G. Zhou, G. Chen, L. Zhao, Investigations for the effects of Ce-substitution on microstructure and magnetic properties of multi-doped YIG ferrites. Ceram. Int. (2025). https://doi.org/10.1016/j.ceramint.2025.04.347
6. M. Amiri, M. Salavati-Niasari, A. Akbari, Magnetic nanocarriers: evolution of spinel ferrites for medical applications. Adv. Colloid Interface Sci. **265**, 29–44 (2019)
7. O.D. Dastjerdi, H. Shokrollahi, S. Mirshekari, A review of synthesis, characterization, and magnetic properties of soft spinel ferrites. Inorg. Chem. Commun. **153**, 110797 (2023)
8. J.M. Gonçalves, L.V. de Faria, A.B. Nascimento, R.L. Germscheidt, S. Patra, L.P. Hernández-Saravia, J.A. Bonacin, R.A.A. Munoz, L. Angnes, Sensing performances of spinel ferrites MFe_2O_4 (M= Mg, Ni, Co, Mn, Cu and Zn) based electrochemical sensors: a review. Anal. Chim. Acta **1233**, 340362 (2022)
9. X. Ji, C. Shen, Y. Zhao, H. Zheng, Q. Wu, Q. Zhang, L. Zheng, P. Zheng, Y. Zhang, Enhanced electromagnetic properties of low-temperature sintered NiCuZn ferrites by doping with Bi_2O_3. Ceram. Int. **48**, 20315–20323 (2022)
10. P. Wang, P. Wang, J. Wang, S. Lv, J. Wang, H. Zheng, Enhancing electromagnetic properties of NiCuZn ferrites through Nb and Li co-doping for wireless power transfer. Ceram. Int. **50**, 54966–54975 (2024)
11. F. Xu, D. Zhang, G. Wang, H. Zhang, Y. Yang, Y. Liao, L. Jin, Y. Rao, J. Li, F. Xie, Influence of LZN nanoparticles on microstructure and magnetic properties of bi-substituted LiZnTi low-sintering temperature ferrites. Ceram. Int. **45**, 1946–1949 (2019)
12. X. Zhou, J. Wang, D. Yao, The effect of Dy and Cu doping on structure and magnetic properties of LiZn ferrites. J. Alloy. Compd. **1022**, 179552 (2025)
13. M. Yang, L. Jia, L. Xu, P. Yi, Y. Shen, W. Fu, Z. Chen, Zn-Ti co-substituted LiZn microwave ferrites: sintering characteristics and gyromagnetic properties. J. Magn. Magn. Mater. **600**, 172171 (2024)
14. J. Li, Y. Yang, G. Wang, L. Guo, Y. Rao, G. Gan, H. Zhang, Enhanced structure and microwave magnetic properties of MgZn ferrite by Cd^{2+} ion substitution for LTCC applications. Ceram. Int. **46**, 6600–6604 (2020)
15. M. Matters-Kammerer, U. Mackens, K. Reimann, R. Pietig, D. Hennings, B. Schreinemacher, R. Mauczok, S. Gruhlke, C. Martiny, Material properties and RF applications of high k and ferrite LTCC ceramics. Microelectron. Reliab. **46**, 134–143 (2006)
16. J.R. Bray, K.T. Kautio, L. Roy, Characterization of an experimental ferrite LTCC tape system for microwave and millimeter-wave applications. IEEE Trans. Adv. Packag. **27**, 558–565 (2004)
17. S.H. Hong, J.H. Park, Y.H. Choa, J. Kim, Magnetic properties and sintering characteristics of NiZn (Ag, Cu) ferrite for LTCC applications. J. Magn. Magn. Mater. **290**, 1559–1562 (2005)
18. U. Ullah, N. Mahyuddin, Z. Arifin, M.Z. Abdullah, A. Marzuki, Antenna in LTCC technologies: a review and the current state of the art. IEEE Antennas Propag. Mag. **57**, 241–260 (2015)
19. P. Guzdek, J. Kulawik, K. Zaraska, A. Bieńkowski, NiZnCu ferrite applied for LTCC microinductor. J. Magn. Magn. Mater. **322**, 2897–2901 (2010)
20. H. Yang, F. Xu, Y. Liao, Y. Ren, G. Liu, Y. Yang, X. Wang, B. Dai, Enhanced gyromagnetic properties of Cu-substituted LiZnTi ferrites for LTCC applications. Ceram. Int. **48**, 20090–20095 (2022)
21. X. Wang, K. Yin, T. Cao, Y. Liao, Z. Wang, Q. Kou, D. Cheng, Effects of Bi_2O_3-V_2O_5 mixture on microstructure and magnetic properties for $Li_{0.42}Zn_{0.27}Ti_{0.11}Mn_{0.1}Fe_{2.1}O_4$

ferrites sintered at low temperatures. J. Alloy. Compd. **885**, 160983 (2021)
22. M. Mahmoudi, M. Kavanlouei, Temperature and frequency dependence of electromagnetic properties of sintering Li–Zn ferrites with nano SiO_2 additive. J. Magn. Magn. Mater. **384**, 276–283 (2015)
23. X. Wang, Z. Zhong, Z. Chen, H. Zhang, Y. Li, C. Liu, J. Li, Y. Liao, Effects of B_2O_3-Li_2CO_3-SiO_2-ZnO glass on properties of $Li_{0.43}Zn_{0.27}Ti_{0.13}Fe_{2.17}O_4$ ferrites sintered at low temperatures. Ceram. Int. **46**, 5719–5724 (2020)
24. K.D. Martinson, I.B. Panteleev, K.A. Steshenko, V.I. Popkov, Effect of Bi_2O_3 contents on magnetic and electromagnetic properties of LiZnMn ferrite ceramics. J. Eur. Ceram. Soc. **42**, 3463–3472 (2022)
25. C. Liu, Z. Lan, X. Jiang, Z. Yu, K. Sun, L. Li, P. Liu, Effects of sintering temperature and Bi2O3 content on microstructure and magnetic properties of LiZn ferrites. J. Magn. Magn. Mater. **320**, 1335–1339 (2008)
26. T. Zhou, H. Zhang, C. Liu, L. Jin, F. Xu, Y. Liao, N. Jia, Y. Wang, G. Gan, H. Su, Li_2O-B_2O_3-SiO_2-CaO-Al_2O_3 and Bi_2O_3 co-doped gyromagnetic $Li_{0.43}Zn_{0.27}Ti_{0.13}Fe_{2.17}O_4$ ferrite ceramics for LTCC Technology. Ceram. Int. **42**, 16198–16204 (2016)
27. Y. Liao, Y. Wang, Z. Chen, X. Wang, J. Li, R. Guo, C. Liu, G. Gan, G. Wang, Y. Li, Microstructure and enhanced magnetic properties of low-temperature sintered LiZnTiMn ferrite ceramics with Bi_2O_3-Al_2O_3 additive. Ceram. Int. **46**, 487–492 (2020)
28. H. Goodarzi, M. Sobhani, Preparation and properties of CaO-added Mn-Zn ferrite ceramic. Ceram. Int. **49**, 36700–36705 (2023)
29. X. Wang, K. Xu, D. Cheng, X. Feng, Enhanced properties of $Li_{0.42}Zn_{0.27}Ti_{0.11}Mn_{0.1}Fe_{2.1}O_4$ ferrites co-fired with Bi_2O_3-B_2O_3 additive at low sintering temperatures. Ceram. Int. **49**, 39465–39472 (2023)
30. F. Xu, X. Shi, Y. Yang, J. Li, Y. Liao, J. Hu, Enhanced magnetic properties of low temperature sintered LiZnTi ferrite ceramic synthesized through adjusting microstructure. J. Alloy. Compd. **827**, 154338 (2020)
31. A.C.F.M. Costa, E. Tortella, M.R. Morelli, R.H.G.A. Kiminami, Synthesis, microstructure and magnetic properties of Ni-Zn ferrites. J. Magn. Magn. Mater. **256**, 174–182 (2003)
32. M.D. Hossain, M.A. Hossain, S.S. Sikder, Hysteresis loop properties of rare earth doped spinel ferrites: a review. J. Magn. Magn. Mater. **564**, 170095 (2022)
33. R. Guo, Z. Yu, Y. Yang, X. Jiang, K. Sun, C. Wu, Z. Xu, Z. Lan, Effects of Bi_2O_3 on FMR linewidth and microwave dielectric properties of LiZnMn ferrite. J. Alloy. Compd. **589**, 1–4 (2014)
34. A. Manzoor, M.A. Khan, W. Kuch, Correlation between ferromagnetic resonance and densification of RE substituted polycrystalline ferrites. Ceram. Int. **44**, 13328–13334 (2018)
35. W. Yang, Y. Qian, H. Zheng, Hot press sintering of Bi-Zn-In-Sn doped yttrium iron garnet ferrite: magnetism, ferromagnetic resonance linewidth and dielectric properties. Ceram. Int. (2025). https://doi.org/10.1016/j.ceramint.2025.03.067
36. K. Liu, Q. Wang, Q. Wu, F. Zhang, L. Li, H. Zheng, Cu-Sn co-doped M-type barium ferrites: magnetism, dielectric properties, and ferromagnetic resonance linewidth. Ceram. Int. (2025). https://doi.org/10.1016/j.ceramint.2025.04.081